



OPEN ACCESS

EDITED BY

Jie Huang,
University of Texas at San Antonio,
United States

REVIEWED BY

Muskhazli Mustafa,
Putra Malaysia University, Malaysia
Mansour AL.Haddabi,
Sultan Qaboos University, Oman

*CORRESPONDENCE

Diana Jumbo-Flores,
✉ djumbo07@utpl.edu.ec

RECEIVED 06 November 2025

REVISED 04 February 2026

ACCEPTED 09 February 2026

PUBLISHED 20 February 2026

CITATION

Jumbo-Flores D, Tillaguango N,
Guerrero K, Moncayo E, Vizúete K,
Debut A, Solano-González S, Omoregie A
and Aguirre P (2026) Enhancing stability of
sandy, clayey, and silty soils through
microbial biostabilization with
Sporosarcina pasteurii.
Front. Environ. Sci. 14:1741098.
doi: 10.3389/fenvs.2026.1741098

COPYRIGHT

© 2026 Jumbo-Flores, Tillaguango,
Guerrero, Moncayo, Vizúete, Debut,
Solano-González, Omoregie and Aguirre.
This is an open-access article distributed
under the terms of the [Creative Commons
Attribution License \(CC BY\)](https://creativecommons.org/licenses/by/4.0/). The use,
distribution or reproduction in other
forums is permitted, provided the original
author(s) and the copyright owner(s) are
credited and that the original publication
in this journal is cited, in accordance with
accepted academic practice. No use,
distribution or reproduction is permitted
which does not comply with these terms.

Enhancing stability of sandy, clayey, and silty soils through microbial biostabilization with *Sporosarcina pasteurii*

Diana Jumbo-Flores^{1*}, Nancy Tillaguango², Karlo Guerrero³,
Eduardo Moncayo^{4,5}, Karla Vizúete⁶, Alexis Debut⁶,
Stefany Solano-González⁷, Armstrong Omoregie⁸ and
Paulina Aguirre¹

¹Grupo de Investigación en Materiales y Ambiente (GIMA), Departamento de Química, Universidad Técnica Particular de Loja, Loja, Ecuador, ²Carrera de Ingeniería Ambiental, Universidad Técnica Particular de Loja, Loja, Ecuador, ³Departamento de Biotecnología, Universidad Tecnológica Metropolitana, Santiago, Chile, ⁴Grupo de Investigación y Desarrollo de la Biotecnología BioSin - Biociencias, Quito, Ecuador, ⁵Carrera de Biotecnología, Escuela Superior Politécnica Agropecuaria de Manabí Manuel Félix López, El Morro, Ecuador, ⁶Centro de Nanociencia y Nanotecnología, Universidad de las Fuerzas Armadas ESPE, Sangolquí, Ecuador, ⁷Laboratorio de Bioinformática Aplicada, Escuela de Ciencias Biológicas, Universidad Nacional, Heredia, Costa Rica, ⁸Centre for Borneo Regionalism and Conservation, University of Technology Sarawak, Sibú, Sarawak, Malaysia

Introduction: Soil degradation and landslide susceptibility represent major environmental challenges in steep terrains affected by inadequate soil management. Microbial-induced carbonate precipitation (MICP) has emerged as a promising bio-based technique to improve soil stability; however, comparative evaluations across different soil textures remain limited.

Methods: This study investigates the application of MICP using *Sporosarcina pasteurii* to improve sandy, silty, and clayey soils collected from active slopes in Loja, Ecuador. Physicochemical, microstructural, and geomechanical properties were evaluated before and after treatment using carbonate quantification, ion exchange analysis, Atterberg limits, direct shear tests, scanning electron microscopy, and energy-dispersive X-ray spectroscopy.

Results: Calcium carbonate precipitation was detected in all soil types, with higher accumulation in finer-textured soils. Exchangeable calcium increased markedly, while sodium decreased in sandy and clayey soils, indicating ion exchange associated with carbonate cementation. The plasticity index decreased in all soils, with reductions of up to ~65% in clayey samples. Geomechanical testing showed consistent improvements, with cohesion increasing by approximately 25–35% in sandy and clayey soils and exhibiting a pronounced relative increase in silty soils. The internal friction angle increased by approximately 30–100%, depending on soil texture. Microstructural analyses confirmed the formation of calcite and vaterite bridging soil particles.

Discussion: Unlike most previous MICP studies focused on a single soil type, this work demonstrates that soil texture strongly governs both the magnitude and

mechanisms of MICP-induced improvement. The results support the potential of MICP as a sustainable and environmentally friendly strategy for near-surface slope stabilization in heterogeneous natural soils.

KEYWORDS

carbonate precipitation, landslide mitigation, MICP, slope stability, soil biostabilization, soil cohesion, *Sporosarcina pasteurii*

1 Introduction

Soil degradation and slope instability represent major environmental challenges worldwide, particularly in regions characterized by steep topography, intense rainfall, and inadequate land management. Globally, soil degradation affects approximately 1.9 billion hectares, with nearly one-third classified as severely degraded, resulting in annual economic losses estimated at 18–20 trillion USD (Ahmad and Pandey, 2018). In Ecuador, more than half of the national territory is affected by degradation processes, with particularly severe impacts in agricultural and mountainous regions such as El Oro, Loja, Azuay, Manabí, Chimborazo, and Tungurahua (Ochoa-Cueva et al., 2015; León et al., 2020).

In Loja Province, erosion susceptibility is especially critical, with approximately 86% of the territory classified as highly vulnerable due to steep slopes, frequent rainfall, artificial embankments, land-use changes, and inadequate soil management practices (Municipio de Loja, 2020). These conditions not only reduce soil productivity but also significantly increase the likelihood of slope failures and landslides, posing risks to infrastructure, ecosystems, and local communities (Pennock, 2019). Landslide occurrence is controlled by a combination of triggering factors, including erosion, extreme precipitation, seismic activity, and anthropogenic disturbances, all of which contribute to reductions in soil shear strength and slope stability (Alexander, 1992; Hongde et al., 2021; Chandler, 2020).

Conventional slope stabilization techniques, such as the use of lime, cement, and other inorganic binders, aim to improve soil strength by modifying physical and chemical properties. While effective, these approaches are often associated with high economic costs, intensive energy consumption, and significant greenhouse gas emissions, raising concerns regarding their long-term environmental sustainability (Behnood, 2018; Zhang et al., 2010; Özen and Şimşek, 2015).

In response to these limitations, microbially induced carbonate precipitation (MICP) has emerged as a promising biotechnological alternative for soil improvement. This process relies on urease-producing microorganisms to induce calcium carbonate precipitation, which acts as a natural cementing agent, enhancing soil strength and stiffness while reducing porosity (Dejong et al., 2014; Umar et al., 2016). Due to its relatively low energy demand and reduced environmental footprint, MICP is increasingly regarded as an eco-friendly and sustainable soil stabilization technique (Omoregie et al., 2021).

A critical factor for effective MICP treatment is the presence of active microorganisms that provide nucleation sites for calcium carbonate precipitation (Osinubi et al., 2019). Among the bacteria investigated, *Sporosarcina pasteurii* has been widely recognized for its high urease activity and efficiency in inducing carbonate precipitation (Lapierre and Huber, 2024; Dong et al., 2023; Hadi et al., 2022). Through urea hydrolysis, *S. pasteurii* increases pore-water pH and carbonate availability, promoting calcium carbonate

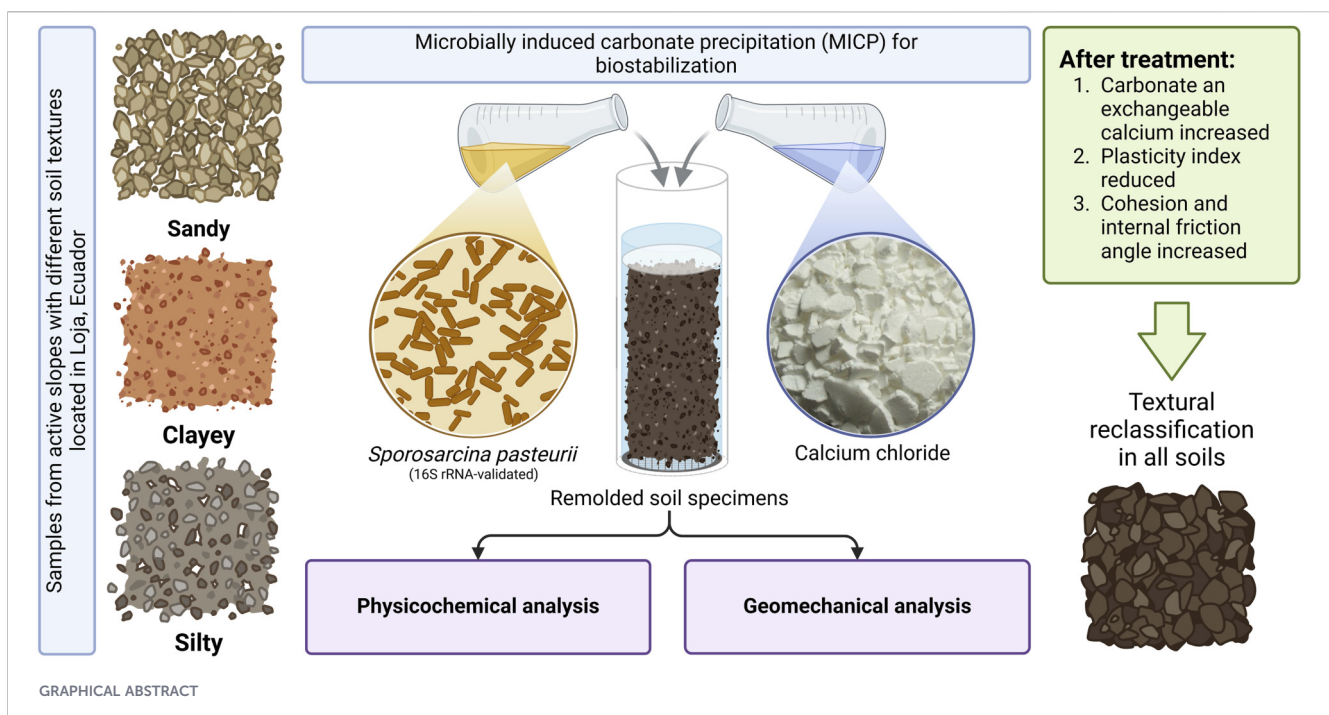


TABLE 1 Sampling points and coordinates for the different soil types in Loja, Ecuador.

| Texture | Sector | Length (m) | Latitude | Altitude (m.a.s.l.) |
|---------|--------------------------------|------------|----------|---------------------|
| Sandy | Colinas Lojanas | 697177 | 9555192 | 2304 |
| Silty | Urbanización de los Operadores | 699880 | 9552704 | 2166 |
| Clayey | Capulí | 699880 | 9552692 | 2154 |



formation that enhances soil cohesion and shear resistance (Safdar et al., 2021). As a result, MICP has shown considerable potential for slope stabilization and erosion mitigation (Mujah et al., 2017).

Despite the growing body of research on MICP using *Sporosarcina pasteurii*, most existing studies focus on a single soil type—commonly sands—or evaluate mechanical improvements without systematically comparing the response of different soil textures. Consequently, the influence of soil texture on the coupled physicochemical and mechanical mechanisms governing MICP-treated soils remains insufficiently understood. This limitation is particularly relevant for natural slope environments, where soil heterogeneity and contrasting particle size distributions directly affect carbonate precipitation, interparticle bonding, and shear resistance, thereby constraining the transferability of laboratory-scale MICP results to field-scale slope stabilization.

To address this research gap, the present study evaluates the effectiveness of MICP using *Sporosarcina pasteurii* for the biostabilization of slopes composed of sandy, silty, and clayey soils collected from active slopes in Loja, Ecuador. Through a comprehensive set of physical, chemical, microstructural, and geomechanical analyses, this work investigates texture-dependent changes in carbonate precipitation, ion exchange behavior, plasticity, cohesion, and internal friction angle. By explicitly

comparing contrasting soil textures under controlled MICP conditions, this study aims to clarify the role of soil type in MICP performance and to assess its potential as a sustainable approach for enhancing near-surface slope stability in erosion-prone regions.

2 Materials and methods

2.1 Soil sample acquisition

The study was conducted on three artificial, homogeneous, and active slopes with different soil textures (sandy, clayey, and silty) located in Loja, Ecuador. Soil samples were collected from selected locations, ensuring representation of distinct textural classes. The specific sampling points, including coordinates and altitude, are detailed in Table 1.

To provide a visual representation of the sampling sites, Figure 1 presents a georeferenced map indicating the exact locations of soil collection.

The soil sampling procedure followed the NTE INEN-ISO 10381–2 standard for soil quality and sampling. In the central section of each slope, the vegetation cover was removed, and

disturbed soil samples were collected from a depth of 30 cm using a shovel. Approximately 6 kg of soil was extracted from each site. Additionally, undisturbed soil samples were taken in accordance with ASTM D4220. All samples were placed in labeled plastic bags and transported to the Soil Chemistry Laboratory at Universidad Técnica Particular de Loja for further analysis.

2.2 Isolation, molecular identification, and phylogenetic analysis of ureolytic bacteria

The bacterium used in this study, *Sporosarcina pasteurii*, was isolated from samples collected at a wastewater treatment plant in Manta, Ecuador. A total of 2 kg of sludge was obtained from both the influent and effluent sections of the plant. The sludge samples were collected using sterile tools, placed in sterile plastic bags, properly sealed, and stored in an ice box at temperatures below 4 °C during transportation to the laboratories of the Universidad Técnica Particular de Loja.

The enrichment culture technique was used to isolate urease-producing bacteria, following the procedure described by Omoregie et al. (2016). The isolated strains were identified through molecular characterization.

Genomic DNA from the isolated bacterial strains was extracted using The Wizard® Purification Kit (Promega, United States). Universal primers 27F and 1492R (Baker et al., 2003) were employed to amplify the 16S rRNA region, and the resulting amplicons were sent to Macrogen (Seoul, Republic of Korea) for Sanger sequencing. Raw sequencing data were manually curated to remove adapters and low-quality nucleotides. The processed sequences were analyzed using the EzTaxon-e server (<https://www.ezbiocloud.net>), and closely related sequences (96% threshold) were downloaded (Chalita et al., 2024). Sequence alignments were performed using MAFFT v.7.397 (Katoh et al., 2002), and the best-scoring maximum likelihood (ML) phylogenetic tree was constructed using IQ-tree 2.2.0-beta with the -m MFP option. Phylogenetic relationships were inferred, and topological robustness was evaluated with 10,000 ultrafast bootstrap replicates (-bb 10,000). The resulting phylogenetic trees were visualized with ITOL v.6 (<https://itol.embl.de/>).

Additionally, phylogenetic distances were calculated using the p-distance model. Ambiguous positions were removed using the pairwise deletion method, resulting in a final dataset comprising 1483 positions. All evolutionary analyses were performed using MEGA11.

2.3 Soil characterization

Disturbed soil samples were air-dried at room temperature (25 °C) for 48 h, then sieved and homogenized using a No. 10 sieve (AS 200, RETSCH, Germany) to achieve a particle size smaller than 2 mm, based on the soil's textural class, targeting the fine fraction.

Soil pH was measured following ASTM D4972 with a 1:2 mass-to-volume ratio using a Seven Easy pH meter (Mettler Toledo, Switzerland). Carbonate content was determined by titration (GLOSOLAN-SOP-05). Soil texture was analyzed via the Bouyoucos method using a vertical agitator (H-4260A, Hamilton Beach, United States) (Bouyoucos, 1936). Exchangeable bases (Na⁺,

K⁺, Ca²⁺, and Mg²⁺) were measured using the US EPA 3052 method, employing a flame atomic absorption spectrometer (AA400, Perkin Elmer, United States). Cation exchange capacity (CEC) was measured using the ammonium acetate saturation method (Chapman, 1965).

For undisturbed samples, moisture content was determined according to AASHTO T 265. The Atterberg limits were determined in accordance with AASHTO T089-96 for the liquid limit (LL) and AASHTO T090-96 for the plastic limit (PL). The plasticity index (PI) was then calculated as the difference between the liquid limit and the plastic limit, as follows:

$$PI = LL - PL$$

Particle size distribution was analyzed according to the Unified Soil Classification System (USCS) following ASTM D422. Triaxial compression tests, performed per AASHTO T234, determined soil cohesion and internal friction angle using remolded specimens (5 cm diameter, 10 cm height) in a triaxial apparatus (Wykeham Farrance, TRITECH, UK).

2.4 Microbial induction of calcite precipitation

To evaluate the effect of microbially induced calcite precipitation (MICP), the *Sporosarcina pasteurii* strain isolated in this study was used. The bacteria were cultured in 500 mL Erlenmeyer flasks containing 100 mL of a liquid medium composed of Nutrient Broth (M002, HiMedia Laboratories Pvt. Ltd., India) and 2% urea, as commonly used for the cultivation of *Sporosarcina pasteurii* in MICP applications (Gat et al., 2014). The flasks were incubated overnight in an orbital shaker (Qmax 3000, Thermo Scientific, United States) at 30 °C and 180 rpm to obtain sufficient biomass for inoculation.

For carbonate precipitation tests, a solution containing 1 N calcium chloride (CaCl₂) as the calcium source was prepared, following the procedure described by Cheng et al. (2014). Remolded soil specimens were prepared using PVC molds (5 cm diameter, 10 cm height). These specimens were inoculated twice with the isolated *Sporosarcina pasteurii* strain, at 0 and 24 h, respectively.

The volumes of inoculum and cementing solution applied to each soil specimen varied according to the soil's textural class, Atterberg limits, and initial moisture content under normal conditions (Table 2). The initial cell concentration was adjusted to 2×10^8 cells/mL, as verified by Neubauer chamber counting (0.02 mm depth), ensuring a consistent microbial load across treatments.

To ensure comparability among soils with different textures, a single bacterial concentration was used in all experiments. This approach allows the influence of soil texture and pore structure on MICP-induced carbonate precipitation to be evaluated independently, while avoiding confounding effects associated with variable microbial inoculation levels (Cheng et al., 2013).

All experiments were conducted using independent soil specimens treated under identical conditions. The bacterial inoculum was prepared from a single microbial culture and used for all treatments; therefore, the replicates represent independent experimental (technical) replicates rather than independent biological replicates. This design was selected to reduce biological variability and to isolate the effects of soil texture and treatment conditions on MICP performance.

TABLE 2 Volumes of initial moisture, liquid limit, inoculum, and cementing solution applied to each soil type.

| Texture | Initial moisture (mL) | Liquid limit (mL) | Maximum volume (mL) | Inoculum (mL) | CaCl ₂ (mL) |
|---------|-----------------------|-------------------|---------------------|---------------|------------------------|
| Sandy | 16.94 | 51.28 | 34.34 | 17.17 | 17.17 |
| Silty | 33.60 | 51.29 | 17.69 | 8.85 | 8.85 |
| Clayey | 18.14 | 51.29 | 33.15 | 16.57 | 16.57 |

The specimens were left to react for 14 days, after which the following parameters were quantified: cation exchange capacity (CEC), carbonates, exchangeable bases (Na⁺, K⁺, Ca²⁺, and Mg²⁺), pH, electrical conductivity, texture, Atterberg limits, and triaxial compression tests.

The curing period was set to 14 days, as previous studies have demonstrated that MICP-treated soils typically reach their maximum mechanical strength and stable carbonate cementation within this timeframe. Earlier curing stages show limited strength development due to incomplete calcium carbonate precipitation, whereas strength gains beyond 14 days tend to plateau as microbial activity decreases and cementation stabilizes (Omeregbe et al., 2024; Wu et al., 2024; Payan et al., 2024).

2.5 Scanning electron microscopy (SEM) analysis

To verify calcium carbonate precipitation and assess bacterial cementation, a soil sample from the MICP-treated group was analyzed using scanning electron microscopy (SEM). The sample was mounted on an aluminum stub with carbon tape, sputter-coated with gold, and examined using a Tescan Mira 3 SEM (Tescan, Czech Republic) equipped with an energy-dispersive X-ray spectroscopy (EDS) detector.

Secondary electron images were captured at an accelerating voltage of 5 kV to visualize the morphological characteristics of the calcium carbonate deposits and bacterial-induced cementation. EDS analysis was performed with a Bruker X-Flash 6–30 detector (Bruker, Germany) operating at 25 kV to determine the elemental composition of the precipitates.

2.6 Replication and data processing

All experiments in this study were conducted in triplicate, with duplicate analytical measurements ($n = 6$). Data were analyzed before and after treatment, and results are expressed as the mean \pm standard error of the mean (SEM). Statistical analysis was performed using a two-way ANOVA with a significance level set at $p \leq 0.05$, conducted with Prism GraphPad Version 9.5.1.

3 Results

3.1 Molecular identification and phylogenetic analysis

The EzTaxon-e server was used to identify the bacterial isolates by searching against quality-controlled databases of 16S rRNA

sequences. The top hit strain for both A1 and E4 sequences (Accession numbers PV173707 and PV173706, respectively) was *Sporosarcina pasteurii* (strain NCIMB 8841) with 100% and 99.57% identity, respectively.

To construct a 16S rRNA phylogeny, 30 bacterial sequences sharing at least 96% identity with A1 and E4 isolates were downloaded. The resulting maximum likelihood (ML) tree (Figure 2) shows that A1 and E4 form a distinct clade within a cluster containing *Sporosarcina pasteurii* NCIMB 8841T. This phylogenetic placement, supported by the bootstrap values shown in the same figure, confirms the assignment of A1 and E4 to the genus *Sporosarcina*. A similar phylogenetic arrangement has been previously reported by Sun et al. (2017). This finding is further supported by genetic distances calculated (Supplementary Figure S1), where a low distance was observed between *S. pasteurii* and A1 and E4 isolates.

3.2 Changes in pH and carbonate content following soil biostabilization

Soil pH plays a crucial role in microbially induced calcite precipitation (MICP), influencing carbonate formation and overall soil stability. As shown in Figure 3A, pH increased significantly in sandy and clayey soils after biostabilization. Specifically, sandy soils exhibited a mean pH increase of approximately 1 unit (from 5.43 ± 0.116 to 6.15 ± 0.045), while clayey soils showed a more pronounced increase of nearly 2 units (from 6.01 ± 0.027 to 7.92 ± 0.069). In contrast, silty soils exhibited a pH decrease of approximately 2 units (from 7.54 ± 0.263 to 5.12 ± 0.048), suggesting a different biochemical response to the treatment. All differences are significant with $p < 0.05$.

Figure 3B presents the carbonate content (CaCO₃) before and after treatment. The results indicate a significant increase in carbonate content across all soil types ($p < 0.05$), though the magnitude of this increase varied. Clayey soils displayed the highest accumulation of carbonates, followed by sandy and silty soils.

3.3 Morphological and elemental characterization of calcium carbonate precipitates

Scanning electron microscopy (SEM) analysis revealed distinct morphological variations in calcium carbonate precipitates formed during microbially induced carbonate precipitation (MICP). Well-defined rhombohedral calcite crystals were the predominant phase, densely packed within the soil matrix, acting as cementing agents that enhanced

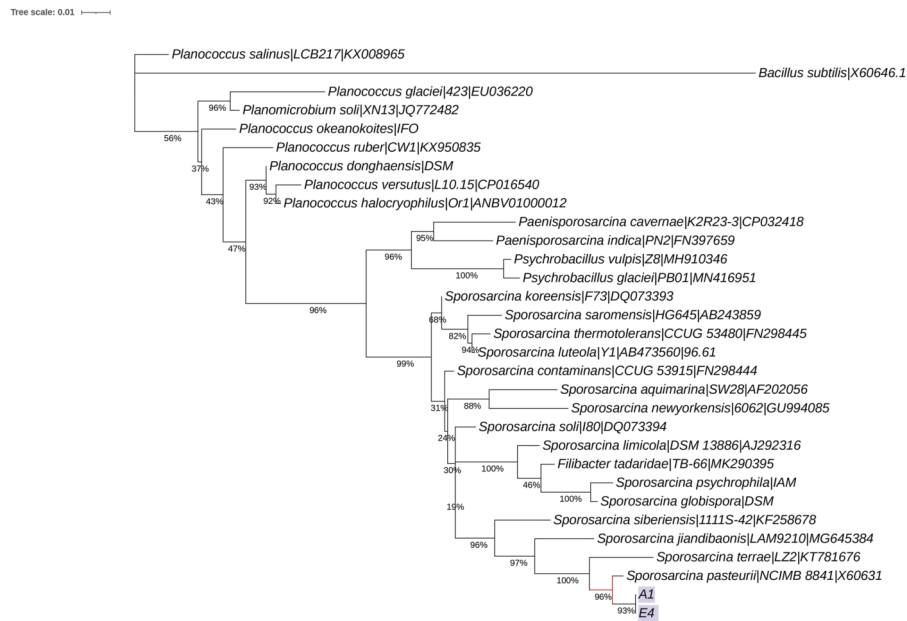


FIGURE 2 Maximum likelihood phylogenetic tree constructed from 16S rRNA sequences of A1 and E4 isolates and closely related bacterial species. The tree was built using MAFFT alignments and the TIM3 + F + I + G4 model in IQ-Tree with 10,000 ultrafast bootstrap replicates. Bootstrap support values are shown as percentages. A1 and E4 cluster with *Sporosarcina pasteurii* NCIMB 8841, supported by high bootstrap values. *Bacillus subtilis* (X60646.1) was used as an outgroup.

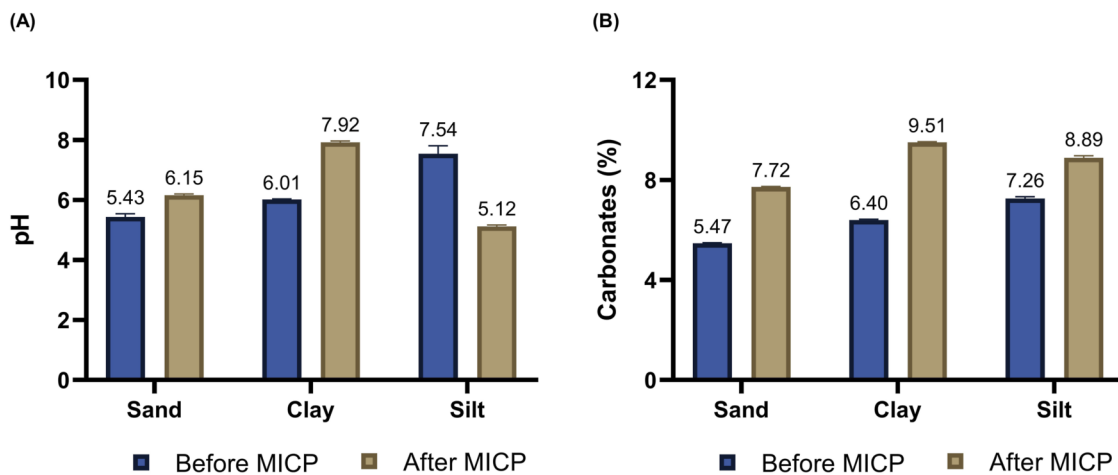


FIGURE 3 Comparative data of pH (A) and carbonates (B) in sandy, clayey, and silty soil samples before and after the biostabilization treatment. Data represent mean values of triplicates \pm SD ($n = 6$).

mechanical stability by binding soil particles together. Additionally, spherical vaterite precipitates of varying sizes were observed, often forming aggregates. This suggests active microbial precipitation with a potential transformation into calcite over time. The coexistence of these distinct morphologies indicates a heterogeneous biomineralization process, influenced by localized microenvironmental conditions that govern the formation of calcium carbonate polymorphs (Figure 4).

3.4 Cation exchange capacity and exchangeable bases

In this study, the cation exchange capacity (CEC) of all three soil types increased after the biostabilization treatment (Figure 5), indicating modifications in their physicochemical properties. These increases were significant with $p < 0.05$.

Clayey soil exhibited the most significant increase in CEC, rising from 0.23 ± 0.022 meq/100 g before treatment to 19.54 ± 0.467 meq/

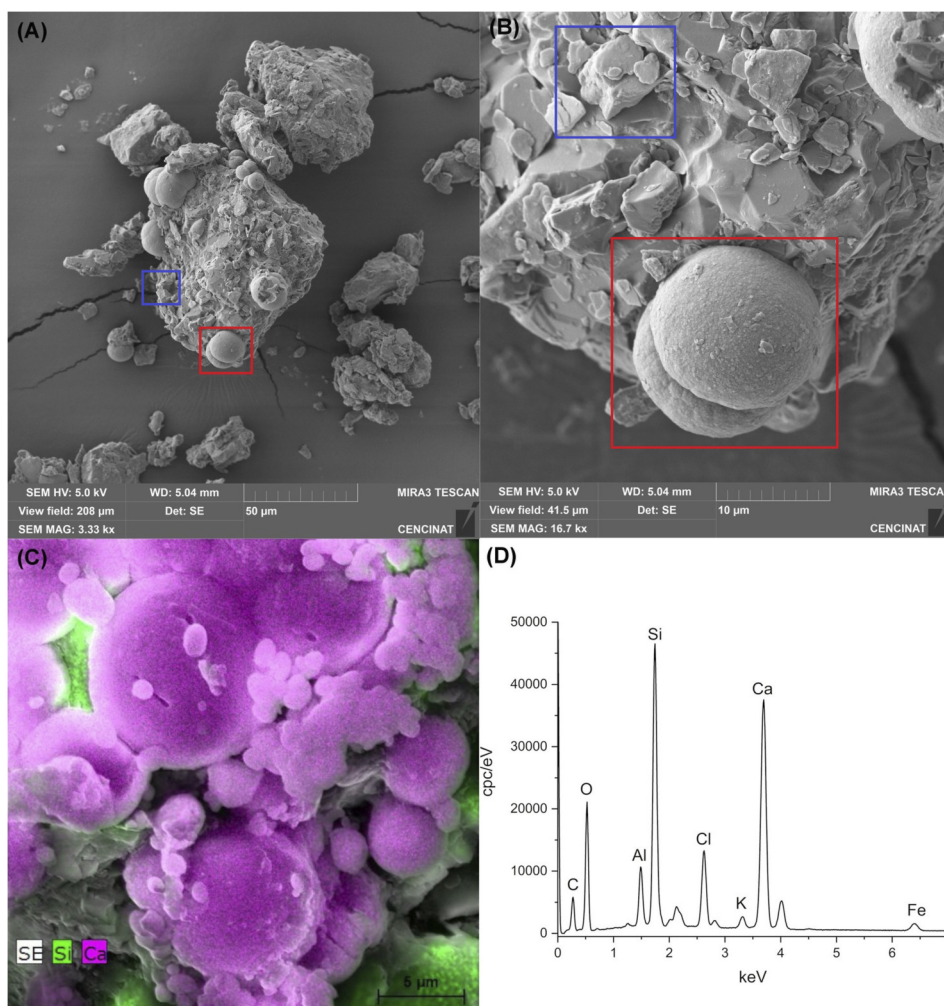


FIGURE 4 Morphological and elemental characterization of calcium carbonate precipitates in biostabilized soil: **(A)** SEM image at $50\ \mu\text{m}$ scale showing soil aggregates with embedded rhombohedral calcite crystals and spherical precipitates, characteristic of calcium carbonate deposition; **(B)** SEM image at $10\ \mu\text{m}$ scale showing spherical vaterite precipitates and rhombohedral calcite crystals attached to the soil matrix; **(C)** EDS elemental mapping highlighting the distribution of calcium (Ca, purple) and silicon (Si, green); **(D)** EDS spectrum showing the elemental composition of the analyzed area.

100 g post-treatment. Similarly, silty soil exhibited an increase in CEC from 2.14 ± 0.053 meq/100 g to 13.54 ± 0.757 meq/100 g. In sandy soil, a more moderate increase in CEC was measured, rising from 3.44 ± 0.136 meq/100 g to 5.89 ± 0.177 meq/100 g.

Regarding exchangeable bases, calcium (Ca^{2+}) concentrations increased significantly ($p < 0.05$) in all soil samples, with initial values ranging from 3116.64 ± 172.31 mg/kg to 6883.89 ± 306.60 mg/kg, reaching up to 62438.26 ± 2080.19 mg/kg after treatment (Figure 6A). Potassium (K^+) also showed a substantial increase (Figure 6C), with final concentrations exceeding 14000 mg/kg, particularly in coarser-textured soils.

Sodium (Na^+) concentrations decreased significantly ($p < 0.05$) in sandy and clayey soils (Figure 6B), with final values below 700 mg/kg. Conversely, a slight increase was recorded in silty soils, reaching a final value of 1537.13 ± 58.8 mg/kg. Magnesium (Mg^{2+}) also exhibited a general decrease across most soils (Figure 6D), with reductions exceeding 50% compared to initial values. However, an increase was observed in silty soils, where

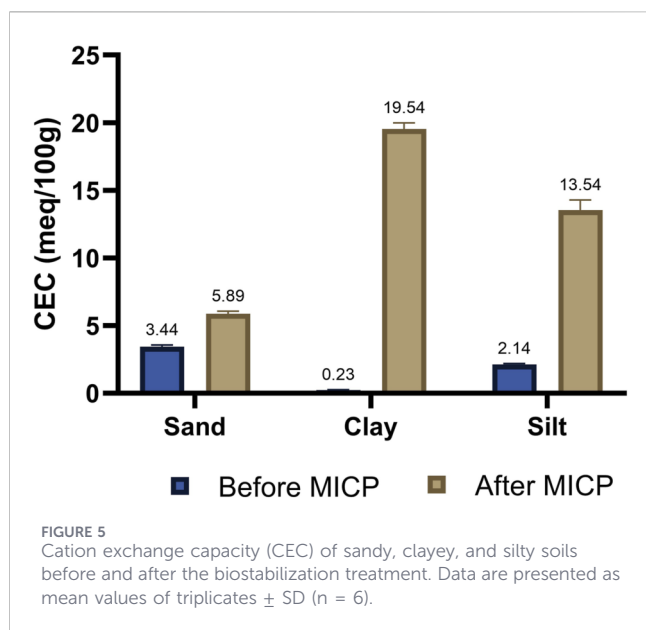
concentrations reached 1820.39 ± 71.74 mg/kg. All differences are significant with $p < 0.05$.

3.5 Textural changes induced by biostabilization

Soil texture was assessed before and after biostabilization. The results (Table 3) show notable modifications in the textural classification of all three soil types following treatment.

Initially, the soils were classified as sandy clay loam, clay loam, and silty loam. After treatment, textural shifts were observed, with the sandy clay loam transitioning to sandy loam, the clay loam to loamy sand, and the silty loam to sandy loam. These changes are associated with variations in the proportions of sand, silt, and clay.

The clay-sized fraction showed an apparent reduction to below the detection limit of the hydrometer analysis in all soil types after MICP treatment, while the sand fraction increased consistently across all samples. In sandy soils, the silt content increased from



$28.8\% \pm 1.44\%$ – $40.75\% \pm 0.04$, contributing to an apparent shift toward a coarser textural classification.

The apparent reduction of the clay-sized fraction after MICP treatment is attributed to particle aggregation and calcium carbonate cementation, which promote the incorporation of fine particles into larger, hydraulically coarser aggregates. These aggregation effects influence sedimentation-based particle size measurements and do not imply clay removal or mineralogical transformation.

The most pronounced transformation occurred in clayey soils, where the clay fraction dropped from $28.9\% \pm 1.11\%$ to 0%, and the sand fraction increased from $41\% \pm 0.83\%$ – $72.48\% \pm 0.81$. This indicates a significant alteration in particle distribution, resulting in a transition to loamy sand. Similarly, silty soils experienced a marked shift, with the clay fraction reduced from $15.4\% \pm 1.10\%$ to 0%, and the sand fraction increasing from $33.4\% \pm 1.03\%$ – $60.00\% \pm 0.01$. This resulted in a reclassification from silty loam to sandy loam.

3.6 Impact of biostabilization on atterberg limits

The Atterberg limits, including the liquid limit (LL) and plastic limit (PL), were measured before and after the biostabilization treatment for sandy, clayey, and silty soils. The Plasticity Index (PI) was then calculated as the difference between LL and PL. The results, presented in Figure 7, show the changes in LL (A), PL (B), and PI (C) across all soil types. These results indicate that the treatment led to an increase in both LL and PL, with varying degrees of change depending on the initial soil composition, while the PI showed a marked reduction for all soil types after treatment. All differences are significant with $p < 0.05$.

The LL increased across all soil types after treatment. Sandy soil exhibited a moderate increase of 11.5% (from 26.12 ± 0.59 to 29.12 ± 1.08), while clayey soil showed a more pronounced rise of 16.2% (from 26.00 ± 0.08 to 30.20 ± 0.37). In silty soil, LL increased by 5.5% (from 30.33 ± 0.1 to 32.00 ± 0.7), indicating a less substantial yet notable change. Similarly, the PL increased consistently across all

soil types, with the most significant change observed in clayey soil, where it rose by 71.8% (from 15.43 to 26.50). In sandy and silty soils, PL increased by 16.6% (from 21.44 to 25.00) and 2.5% (from 27.80 to 28.50), respectively, reflecting modifications in soil plasticity due to the biostabilization treatment.

As a result of these changes, the Plasticity Index (PI), calculated as the difference between LL and PL, showed a marked reduction across all soil types. The most significant decrease was observed in clayey soil, where PI dropped by 65% (from 10.57 ± 0.42 to 3.70 ± 0.71), indicating a substantial reduction in plasticity. In silty and sandy soils, PI decreased by 57% (from 4.20 ± 1.1 to 1.80 ± 0.5) and 12% (from 4.68 ± 0.65 to 3.09 ± 0.56), respectively.

3.7 Mechanical behavior of biostabilized soils

The triaxial compression test was performed to assess the stress-strain response of sandy, clayey, and silty soils before and after biostabilization. This test measured cohesion and the internal friction angle (ϕ), both key parameters in determining soil strength and stability. The obtained results indicate a significant improvement in soil mechanical properties after treatment (Figure 8).

Cohesion increased across all soil types, with sandy and clayey soils increasing from 0.75 to 1.00 kg/cm² and 0.80–1.00 kg/cm², respectively. Silty soil exhibited the most pronounced change, increasing from 0.22 to 2.00 kg/cm². This corresponds to an increase in cohesive forces of 33% in sandy soil, 25% in clayey soil, and 800% in silty soil.

A similar trend was observed in the internal friction angle, which increased from 20° to 41° in sandy soil, 25°–32° in clayey soil, and 25°–34° in silty soil. These increments represent a 100% increase in sandy soil, 28% in clayey soil, and 36% in silty soil.

Large percentage increases should be interpreted in the context of the very low initial shear strength of the untreated soils; therefore, absolute post-treatment values provide a more meaningful indicator of mechanical improvement. While the laboratory results indicate a positive contribution to shear strength, field-scale slope stability depends on site-specific conditions and cannot be directly inferred from laboratory parameters alone.

4 Discussion

The three soil types studied (sandy, silty, and clayey) underwent significant changes in their chemical and mechanical properties as a result of biostabilization. The subsequent subsections will examine these changes individually, providing a detailed analysis of their implications.

4.1 Changes in pH and carbonate content following soil biostabilization

The increase in pH observed in sandy and clayey soils is consistent with the expected MICP mechanism, where urea hydrolysis generates ammonia and hydroxide ions, creating alkaline conditions that favor carbonate precipitation (Safdar et al., 2021). During MICP, urea hydrolysis generates ammonia

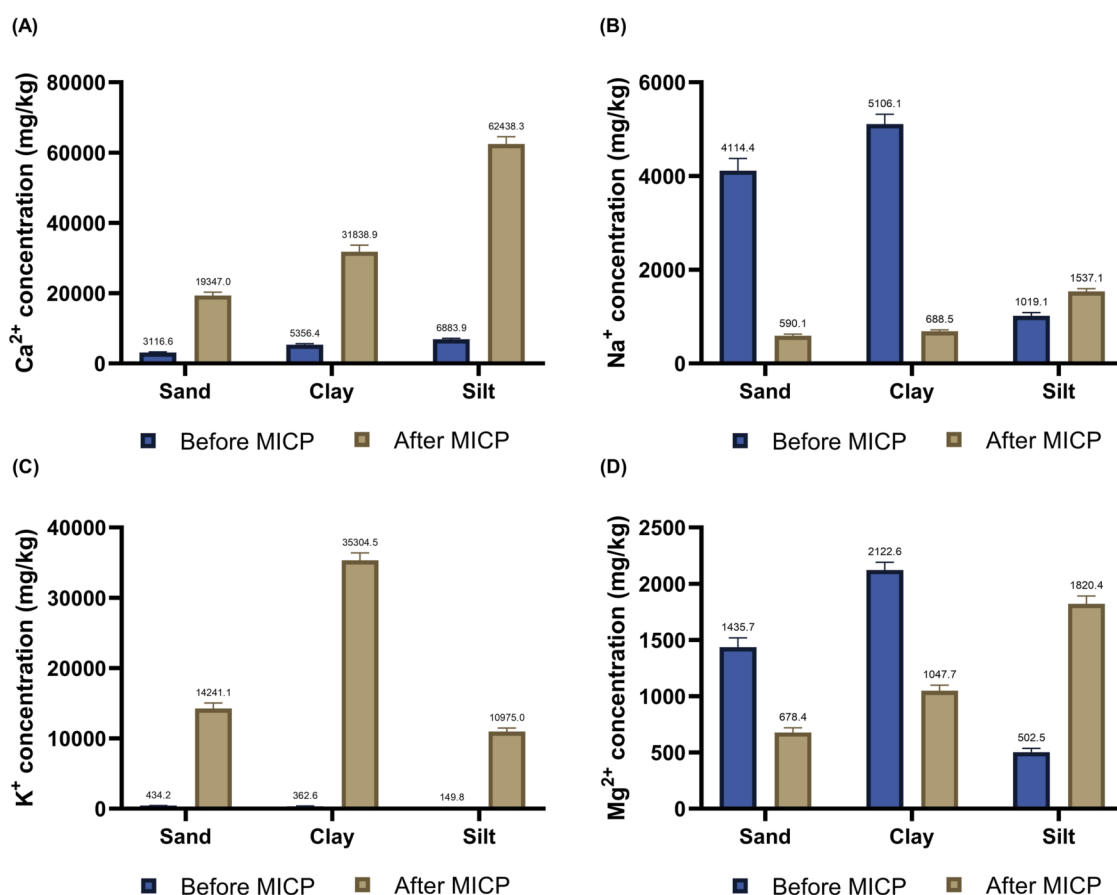


FIGURE 6 Concentrations of exchangeable bases: (A) Ca²⁺, (B) Na⁺, (C) K⁺, and (D) Mg²⁺, in sandy, silty, and clayey soils before and after biostabilization treatment. Data are presented as mean values of triplicates ± SD (n = 6).

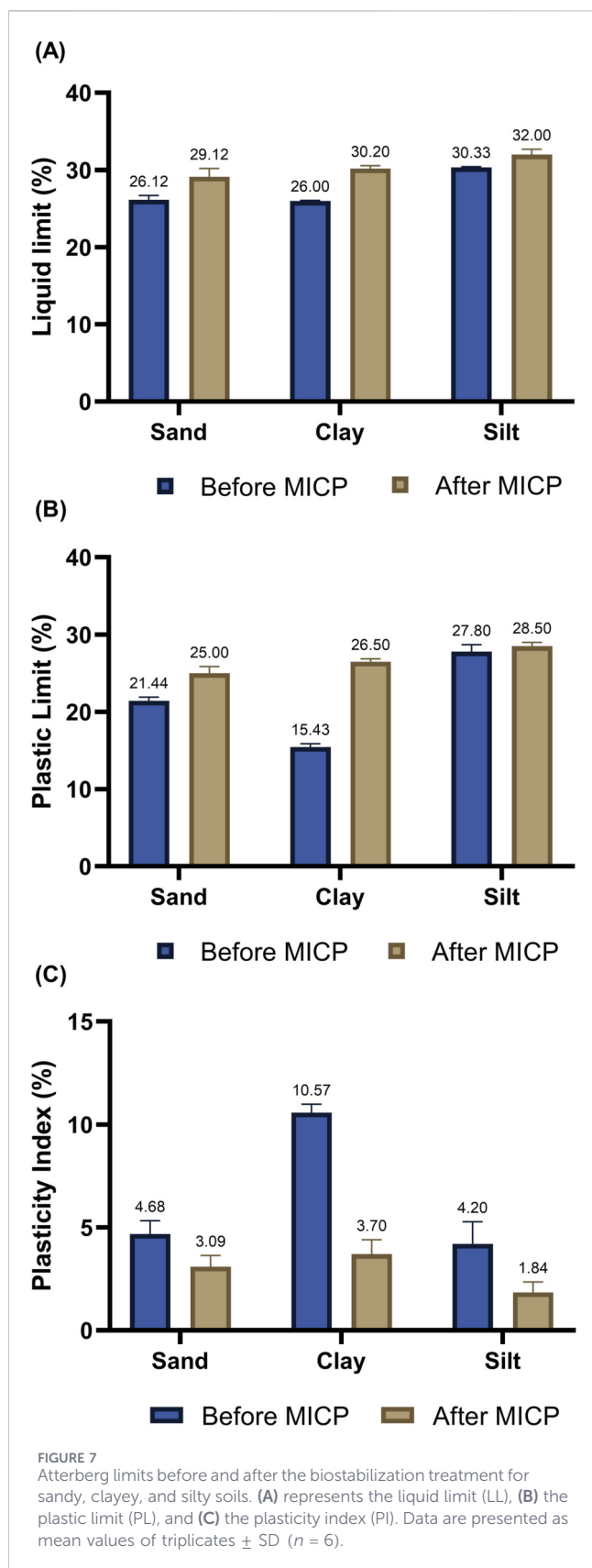
TABLE 3 Textural changes in sandy, silty, and clayey soils before and after biostabilization treatment. Data are presented as mean values of triplicates.

| Soil type | Before treatment | | | | After treatment | | | |
|-----------|------------------|----------|----------|-----------------|-----------------|----------|----------|----------------|
| | Sand (%) | Clay (%) | Silt (%) | Textural class | Sand (%) | Clay (%) | Silt (%) | Textural class |
| Sand | 47.5 | 23.7 | 28.8 | Sandy clay loam | 59.25 | 0 | 40.75 | Sandy loam |
| | ± 1.71 | ± 0.92 | ± 1.44 | | ± 0.04 | 0 | ± 0.04 | |
| Clay | 41.0 | 28.9 | 30.1 | Clay loam | 72.48 | 0 | 27.52 | Loamy sand |
| | ± 0.83 | ± 1.11 | ± 1.03 | | ± 0.81 | 0 | ± 0.88 | |
| Silt | 33.4 | 15.4 | 51.2 | Silty loam | 60.00 | 0 | 40.00 | Sandy loam |
| | ± 1.03 | ± 1.10 | ± 0.82 | | ± 0.01 | 0 | ± 0.09 | |

(NH₃), which further hydrolyzes into ammonium and hydroxide ions (OH⁻), leading to an overall pH increase in the surrounding environment (Stocks-Fischer et al., 1999). The more pronounced pH shift in clayey soils may be attributed to their higher cation exchange capacity, which enhances ion retention and buffering effects, stabilizing alkaline conditions.

In contrast, the pH decrease observed in silty soils suggests an alternative biochemical pathway, likely driven by increased

heterotrophic microbial respiration. This leads to CO₂ and organic acid accumulation, which acidifies the medium (Fang et al., 2018). This finding is consistent with studies by Ferris et al. (2004) and Omoregie et al. (2020), who reported similar acidification effects under anoxic conditions due to bacterial metabolism. The reduced pH in silty soils may indicate a lower urea hydrolysis rate, potentially necessitating bacterial augmentation to sustain MICP



efficiency (Ashraf et al., 2021). Furthermore, the lower pH correlates with a reduced carbonate accumulation in silty soils, suggesting increased carbonate dissolution or shifts in

microbial metabolic activity that may limit overall MICP performance.

Despite the pH decrease in silty soils, the increase in carbonate content across all soil types confirms successful biostabilization. The addition of calcium chloride (CaCl₂) resulted in calcium carbonate (CaCO₃) precipitation, promoting the aggregation of fine particles into coarser structures, modifying the textural class of the soils. This effect was particularly notable in clayey soils, where higher carbonate accumulation contributed to a reduction in clay particles and an increase in coarser fractions. The greater carbonate accumulation in clayey soils is likely due to their finer texture and larger surface area, which promote nucleation and retention of precipitated calcite. Conversely, the lower carbonate content in silty soils may result from enhanced carbonate dissolution under acidic conditions or reduced nucleation efficiency.

4.2 Structural and compositional validation of calcium carbonate precipitates

The mineralogical variations observed in the precipitates confirm that MICP promotes the formation of multiple calcium carbonate polymorphs, influenced by localized microenvironmental conditions. The predominance of rhombohedral calcite suggests that the biomineralization process favors its stabilization as the thermodynamically most stable phase. In contrast, the presence of vaterite in certain regions indicates transient mineralization stages, aligning with previous studies where vaterite often appears as an intermediate phase before transforming into calcite (Anbu et al., 2016; Tourney and Ngwenya, 2009).

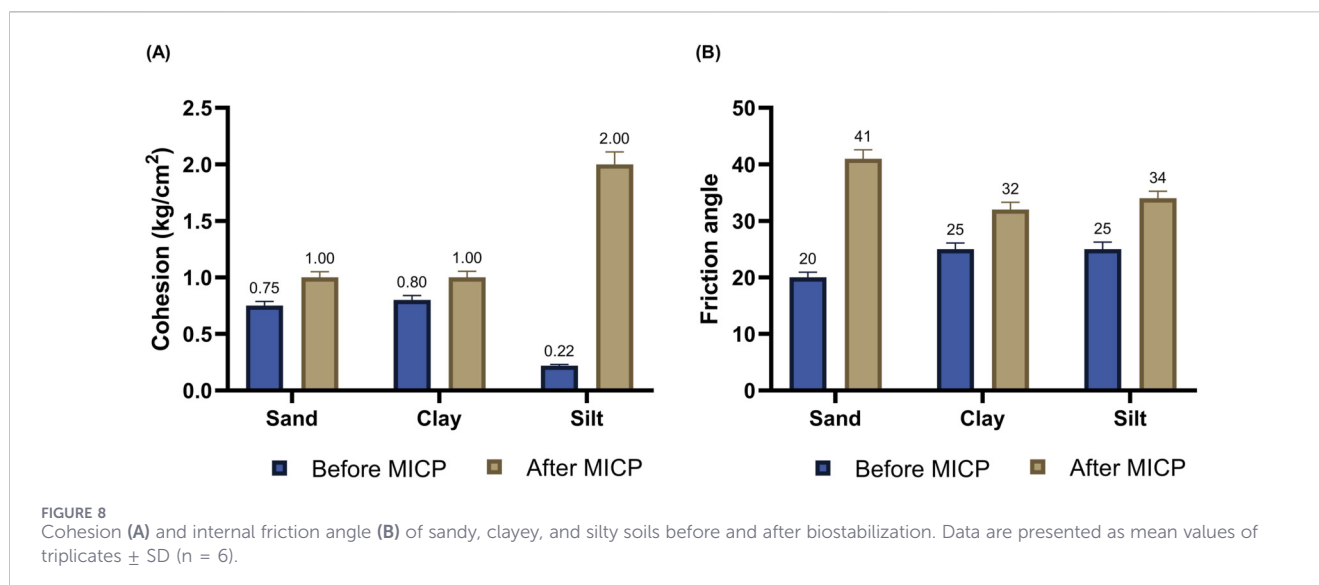
The cementing role of calcite was evident in the formation of dense aggregates binding soil particles, reinforcing its contribution to soil biostabilization. Energy-dispersive X-ray spectroscopy (EDS) confirmed the successful precipitation of calcium carbonate, while also detecting silicon (Si) and aluminum (Al), likely originating from the soil matrix. This suggests that interactions between microbial carbonate precipitation and existing soil components may influence mineralization pathways, potentially affecting the stability and distribution of carbonate phases.

4.3 Cation exchange capacity and exchangeable bases

The cation exchange capacity (CEC) quantifies the ability of soil minerals to adsorb and retain cations, a property closely linked to specific surface area. A higher cation exchange capacity usually enhances soil stabilization by promoting particle aggregation and reducing soil plasticity (Bhurtel et al., 2024).

The increase in CEC after treatment suggests an enhancement in the soil's ability to retain cations, likely due to the incorporation of calcium carbonate and other precipitated minerals. Clayey soils, with their inherently high specific surface area, exhibited the most significant increase in CEC, while sandy soils showed the least improvement due to their lower charge density and larger particle size. The increase in silty soils was also notable, albeit to a lesser extent, reflecting their intermediate texture and surface reactivity.

Regarding exchangeable bases, the marked increase in calcium concentration is directly linked to the addition of



CaCl₂, facilitating calcium adsorption onto soil particles. This corroborates previous studies highlighting the role of calcium in enhancing soil stability through carbonate precipitation (Fu et al., 2023).

Sodium (Na⁺) concentrations decreased in sandy and clayey soils, likely due to cation exchange reactions where calcium (Ca²⁺) replaced sodium (Na⁺) in soil adsorption sites, a well-documented phenomenon in soil stabilization (Ranjbar and Jalali, 2015). However, a slight increase in sodium concentration in silty soils suggests differential ion exchange dynamics influenced by initial soil composition and cation availability.

4.4 Textural changes induced by biostabilization

Soil texture is a key physical property that influences water retention, permeability, and mechanical stability. Textural changes occur when the relative proportions of sand, silt, and clay are altered, affecting soil behavior. Textural changes observed in all soils are attributed to particle aggregation and redistribution driven by MICP. The reduction in clay content suggests that fine particles were incorporated into larger aggregates, shifting the texture toward coarser fractions. In clayey soils, calcium carbonate accumulation likely bound clay particles, effectively reducing the fine fraction and increasing aggregate formation. This effect has been previously reported in soil stabilization studies, where an increase in calcium carbonate (CaCO₃) content leads to an apparent reduction in clay and an increase in coarser particles (Virto et al., 2018).

The apparent reduction of the clay fraction observed after MICP treatment should be interpreted as an effect of particle aggregation and carbonate cementation influencing hydrometer-based measurements, rather than as a true mineralogical alteration or removal of clay minerals. Similar aggregation and contact enhancement effects have been reported in previous MICP studies. For instance, Mahawish et al. (2018) demonstrated that improved particle contacts and cementation significantly affect the mechanical behavior of MICP-treated soils, supporting the

interpretation that particle aggregation, rather than mineralogical alteration, governs the observed changes.

For sandy and silty soils, the increase in the sand fraction may result from the cementation of finer particles into larger aggregates. Calcium carbonate precipitation enhances flocculation and aggregation, leading to reduced clay dispersion and an overall shift toward a coarser texture. This aligns with findings from previous studies on biostabilization, which suggest that calcite formation promotes grain binding and alters soil texture (Xie et al., 2024).

4.5 Impact of biostabilization on atterberg limits

The Atterberg limits include the liquid limit (LL), which defines the transition from a semi-liquid to a plastic state, and the plastic limit (PL), which marks the shift from plastic to semi-solid. The plasticity index (PI), defined as the difference between LL and PL, reflects the soil's plasticity and its response to moisture content variations. Evaluating these limits is essential for understanding the behavior of soils in engineering applications (Shimobe and Spagnoli, 2022).

The increase in LL and PL after biostabilization suggests structural modifications in the soil matrix, likely due to particle aggregation and calcite precipitation. The most significant shift in PL was observed in clayey soils, indicating a reduction in plasticity and a transition toward a more stable structure. The moderate increases of PL in sandy and silty soils indicate that the treatment also affected their ability to retain water at the liquid limit, potentially due to particle aggregation and calcite precipitation.

The reduction in plasticity index across all soil types reflects a transition toward more stable soil behavior under varying moisture conditions. This response is consistent with MICP-induced mechanisms in which calcium carbonate precipitation and associated cation exchange promote clay particle flocculation and pore-space modification, thereby limiting the mobility of fine particles and reducing plastic deformation. Similar reductions in soil plasticity following calcite precipitation have been reported in

previous stabilization studies, where the binding and flocculation of clay minerals contribute to improved mechanical stability (Cokca, 2001).

4.6 Mechanical behavior of biostabilized soils

The mechanical properties of biostabilized soils varied with texture, influencing both cohesion and internal friction angle (ϕ), which exhibited different degrees of enhancement depending on soil type. Friction coefficients correlate with shear resistance, and ϕ typically ranges between 25° and 45° in most soils (Liu et al., 2011). Cohesion, influenced by molecular forces and water films binding soil particles, tends to be higher in finer soils, such as clays (Havaee et al., 2015).

The pronounced increase in cohesion observed in silty soils highlights the texture-dependent effectiveness of MICP, indicating that intermediate-textured materials provide favorable conditions for carbonate precipitation and interparticle bonding. In such soils, calcite formation can efficiently bridge particles and fill pore spaces without the diffusion limitations commonly associated with clay-rich matrices, leading to a more cohesive and mechanically stable soil framework. Similar texture-dependent responses have been reported in previous MICP studies, where silty and fine-grained soils exhibited notable gains in shear strength as a result of effective calcite bonding and pore-scale cementation (Cui et al., 2017; Park et al., 2020).

The biostabilization treatment significantly improved mechanical properties, with cohesion and internal friction angle (ϕ) increasing across all samples, particularly in silty soil, which exhibited the greatest enhancement. These results align with previous studies demonstrating that increased CaCO₃ content enhances soil strength and stiffness (Lin et al., 2016; Wu et al., 2021). In clayey soils, the friction angle reached 32°, and cohesion increased to 1 kg/cm², further confirming the effectiveness of the biostabilization process. This improvement underscores the critical role of CaCO₃ in enhancing soil stability, consistent with findings that even low CaCO₃ concentrations (e.g., 1%) can significantly improve soil resistance (Lin et al., 2016).

Overall, the observed improvements in cohesion and friction angle confirm the effectiveness of biostabilization in enhancing soil stability, supporting its potential application in geotechnical engineering for slope stabilization and erosion control. The mineralogical and compositional analysis further validates the underlying mechanisms driving this stability, demonstrating that microbial carbonate precipitation effectively promotes soil cementation. The combined evidence from SEM and EDS confirms the structural integrity of the precipitated calcium carbonate, reinforcing the role of *Sporosarcina pasteurii* in MICP-based soil stabilization.

While the laboratory-scale results demonstrate the potential of MICP for improving soil mechanical behavior, these findings should be interpreted with caution when considering field-scale slope stability. Although the observed increases in cohesion and shear resistance suggest that MICP can contribute to enhanced near-surface stability and reduced susceptibility to shallow failures, laboratory-derived parameters alone are not sufficient to directly quantify slope stability at the field scale. Field performance is

governed by site-specific factors such as slope geometry, groundwater conditions, treatment depth, spatial uniformity of cementation, and the long-term durability of carbonate bonds.

In addition, the experiments were conducted under controlled conditions that may not fully capture the environmental variability of natural slopes, including fluctuations in moisture, temperature, and long-term biological activity. The use of a single bacterial concentration also does not account for potential texture-specific optimization of microbial dosage. Consequently, future research should focus on field-scale validation, long-term performance assessment, and optimization of MICP treatment parameters. Within this framework, the integrated physicochemical and geomechanical dataset presented in this study provides a soil-specific baseline to support preliminary slope-stability assessments and the design of pilot-scale applications in erosion-prone environments.

5 Conclusion

This study demonstrates that microbially induced carbonate precipitation (MICP) using *Sporosarcina pasteurii* is an effective and environmentally sustainable approach for improving the physicochemical, microstructural, and mechanical behavior of soils derived from active slopes. Across sandy, silty, and clayey soils, MICP promoted calcium carbonate precipitation, enhanced interparticle bonding, increased cohesion and shear resistance, and reduced plasticity in fine-textured soils, thereby contributing to improved structural integrity and slope stability. Microstructural evidence supports that carbonate precipitation in the form of calcite and vaterite contributes to particle aggregation and matrix reinforcement. Overall, the consistent response observed across different soil textures highlights the potential of MICP as a nature-based stabilization strategy for erosion-prone environments; however, further research is required to evaluate its scalability, long-term durability, and performance under field conditions.

Data availability statement

The datasets presented in this study can be found in online repositories. The names of the repository/repository and accession number(s) can be found below: <https://www.ncbi.nlm.nih.gov/genbank/>, PV173706 <https://www.ncbi.nlm.nih.gov/genbank/>, PV173707.

Author contributions

DJ-F: Funding acquisition, Writing – original draft, Resources, Formal Analysis, Project administration, Methodology, Validation, Conceptualization. NT: Investigation, Data curation, Methodology, Writing – review and editing. KG: Formal Analysis, Data curation, Writing – review and editing, Validation. EMO: Writing – review and editing. KV: Writing – review and editing, Investigation. AD: Investigation, Writing – review and editing. SS-G: Methodology, Investigation, Writing – review and editing. AO: Writing – review and editing, Methodology. PA: Validation, Conceptualization,

Writing – review and editing, Investigation, Methodology, Resources, Formal Analysis.

Funding

The author(s) declared that financial support was received for this work and/or its publication. This work was supported by the Universidad Técnica Particular de Loja through the internal call for projects.

Conflict of interest

The author(s) declared that this work was conducted in the absence of any commercial or financial relationships that could be construed as a potential conflict of interest.

Generative AI statement

The author(s) declared that generative AI was not used in the creation of this manuscript.

References

- Ahmad, N., and Pandey, P. (2018). Assessment and monitoring of land degradation using geospatial technology in bathinda district, Punjab, India. *Solid earth*. 9, 75–90. doi:10.5194/se-9-75-2018
- Alexander, D. (1992). On the causes of landslides: human activities, perception, and natural processes. *Environ. Geol. Water Sci.* 20, 165–179. doi:10.1007/bf01706160
- Anbu, P., Kang, C.-H., Shin, Y.-J., and So, J.-S. (2016). Formations of calcium carbonate minerals by bacteria and its multiple applications. *Springerplus* 5, 1–26. doi:10.1186/s40064-016-1869-2
- Ashraf, M. S., Shah, M. U. H., Bokhari, A., and Hasan, M. (2021). Less is more: optimising the biocementation of coastal sands by reducing influent urea through response surface method. *J. Clean. Prod.* 315, 128208. doi:10.1016/j.jclepro.2021.128208
- Baker, G., Smith, J. J., and Cowan, D. A. (2003). Review and re-analysis of domain-specific 16s primers. *J. Microbiological Methods* 55, 541–555. doi:10.1016/j.mimet.2003.08.009
- Behnood, A. (2018). Soil and clay stabilization with calcium-and non-calcium-based additives: a state-of-the-art review of challenges, approaches and techniques. *Transp. Geotech.* 17, 14–32. doi:10.1016/j.trgeo.2018.08.002
- Bhurtel, A., Salifu, E., and Siddiqua, S. (2024). Composite biomediated engineering approaches for improving problematic soils: potentials and opportunities. *Sci. Total Environ.* 914, 169808. doi:10.1016/j.scitotenv.2023.169808
- Bouyoucos, G. J. (1936). Directions for making mechanical analyses of soils by the hydrometer method. *Soil Science* 42, 225–230. doi:10.1097/00010694-193609000-00007
- Chalita, M., Kim, Y. O., Park, S., Oh, H.-S., Cho, J. H., Moon, J., et al. (2024). Ezbiocloud: a genome-driven database and platform for microbiome identification and discovery. *Int. J. Syst. Evol. Microbiol.* 74, 006421. doi:10.1099/ijsem.0.006421
- Chandler, R. (2020). Processes leading to landslides in clay slopes: a review. *Hillslope Process.*, 343–360.
- Chapman, H. (1965). Cation exchange capacity. *Methods Soil Analysis Part 2 Chem. Microbiological Properties*. doi:10.2134/agronmonogr9.2.c6
- Cheng, L., Cord-Ruwisch, R., and Shahin, M. A. (2013). Cementation of sand soil by microbially induced calcite precipitation at various degrees of saturation. *Can. Geotechnical J.* 50, 81–90. doi:10.1139/cgj-2012-0023
- Cheng, L., Shahin, M., Cord-Ruwisch, R., Addis, M., Hartanto, T., Elms, C., et al. (2014). “Soil stabilisation by microbial-induced calcite precipitation (MICP): investigation into some physical and environmental aspects,” in *7th international congress on environmental geotechnics* (Australia: Engineers Australia Melbourne), 64, 1105–1112.
- Cokca, E. (2001). Use of class c fly ashes for the stabilization of an expansive soil. *J. Geotechnical Geoenvironmental Eng.* 127, 568–573. doi:10.1061/(asce)1090-0241(2001)127:7(568)
- Cui, M.-J., Zheng, J.-J., Zhang, R.-J., Lai, H.-J., and Zhang, J. (2017). Influence of cementation level on the strength behaviour of bio-cemented sand. *Acta Geotech.* 12, 971–986. doi:10.1007/s11440-017-0574-9
- Dejong, J. T., Soga, K., Kavazanjian, E., Burns, S., Van Paassen, L., Al Qabany, A., et al. (2014). “Biogeochemical processes and geotechnical applications: progress, opportunities and challenges,” in *Bio-and chemo-mechanical processes in geotechnical engineering: géotechnique symposium in print 2013 (ice publishing)*, 143–157.
- Dong, Y., Gao, Z., Wang, D., Di, J., Guo, X., Yang, Z., et al. (2023). Optimization of growth conditions and biological cementation effect of *Sporosarcina pasteurii*. *Constr. Build. Mater.* 395, 132288. doi:10.1016/j.conbuildmat.2023.132288
- Fang, C., Kumari, D., Zhu, X., and Achal, V. (2018). Role of fungal-mediated mineralization in biocementation of sand and its improved compressive strength. *Int. Biodeterior. and Biodegrad.* 133, 216–220. doi:10.1016/j.ibiod.2018.07.013
- Ferris, F. G., Phoenix, V., Fujita, Y., and Smith, R. (2004). Kinetics of calcite precipitation induced by ureolytic bacteria at 10 to 20 c in artificial groundwater. *Geochimica Cosmochimica Acta* 68, 1701–1710. doi:10.1016/s0016-7037(03)00503-9
- Fu, T., Saracho, A. C., and Haigh, S. K. (2023). Microbially induced carbonate precipitation (MICP) for soil strengthening: a comprehensive review. *Biogeotechnics* 1, 100002. doi:10.1016/j.bgtech.2023.100002
- Gat, D., Tsesarsky, M., Shamir, D., and Ronen, Z. (2014). Accelerated microbial-induced caco 3 precipitation in a defined coculture of ureolytic and non-ureolytic bacteria. *Biogeosciences* 11, 2561–2569. doi:10.5194/bg-11-2561-2014
- Hadi, S., Abbas, H., Almajed, A., Binyahya, A., and Al-Salloum, Y. (2022). Biocementation by *Sporosarcina pasteurii* ATCC6453 under simulated conditions in sand columns. *J. Mater. Res. Technol.* 18, 4375–4384. doi:10.1016/j.jmrt.2022.04.105
- Havaee, S., Mosaddeghi, M., and Ayoubi, S. (2015). *In situ* surface shear strength as affected by soil characteristics and land use in calcareous soils of central Iran. *Geoderma* 237, 137–148. doi:10.1016/j.geoderma.2014.08.016
- Hongde, W., Dongli, S., Xiaoqin, S., Shengqiang, T., and Yipeng, Z. (2021). Analysis of unsaturated shear strength and slope stability considering soil desalinization in a reclamation area in China. *Catena* 196, 104949. doi:10.1016/j.catena.2020.104949
- Katoh, K., Misawa, K., Kuma, K.-i., and Miyata, T. (2002). Mafft: a novel method for rapid multiple sequence alignment based on fast fourier transform. *Nucleic Acids Research* 30, 3059–3066. doi:10.1093/nar/gkf436
- Lapierre, F. M., and Huber, R. (2024). Revisiting the urease production of micp-relevant bacterium *Sporosarcina pasteurii* during cultivation. *Biocatal. Agric. Biotechnol.* 55, 102981. doi:10.1016/j.cbab.2023.102981
- León, M., Alomoto, M., and Barroso, M. d. I. O. (2020). “Analysis of the conservation model of territorial forest and vegetation protection in Azuay, Ecuador,” in *ICAI workshops*, 53–65.

Any alternative text (alt text) provided alongside figures in this article has been generated by Frontiers with the support of artificial intelligence and reasonable efforts have been made to ensure accuracy, including review by the authors wherever possible. If you identify any issues, please contact us.

Publisher’s note

All claims expressed in this article are solely those of the authors and do not necessarily represent those of their affiliated organizations, or those of the publisher, the editors and the reviewers. Any product that may be evaluated in this article, or claim that may be made by its manufacturer, is not guaranteed or endorsed by the publisher.

Supplementary material

The Supplementary Material for this article can be found online at: <https://www.frontiersin.org/articles/10.3389/fenvs.2026.1741098/full#supplementary-material>

- Lin, H., Suleiman, M. T., Brown, D. G., and Kavazanjian, J. (2016). Mechanical behavior of sands treated by microbially induced carbonate precipitation. *J. Geotechnical Geoenvironmental Eng.* 142, 04015066. doi:10.1061/(asce)gt.1943-5606.0001383
- Liu, J., Shi, B., Jiang, H., Huang, H., Wang, G., and Kamai, T. (2011). Research on the stabilization treatment of clay slope topsoil by organic polymer soil stabilizer. *Eng. Geol.* 117, 114–120. doi:10.1016/j.enggeo.2010.10.011
- Mahawish, A., Bouazza, A., and Gates, W. P. (2018). Effect of particle size distribution on the bio-cementation of coarse aggregates. *Acta Geotech.* 13, 1019–1025. doi:10.1007/s11440-017-0604-7
- Mujah, D., Shahin, M. A., and Cheng, L. (2017). State-of-the-art review of biocementation by microbially induced calcite precipitation (MICP) for soil stabilization. *Geomicrobiol. J.* 34, 524–537. doi:10.1080/01490451.2016.1225866
- Municipio de Loja (2020). Plan de desarrollo y ordenamiento territorial del cantón loja: Sociabilización del documento.
- Ochoa-Cueva, P., Fries, A., Montesinos, P., Rodríguez-Díaz, J. A., and Boll, J. (2015). Spatial estimation of soil erosion risk by land-cover change in the andes of southern Ecuador. *Land Degradation and Development* 26, 565–573. doi:10.1002/ldr.2219
- Omeregje, A. I., Senian, N., Li, P. Y., Hei, N. L., Leong, D. O. E., Ginjom, I. R. H., et al. (2016). Ureolytic bacteria isolated from Sarawak limestone caves show high urease enzyme activity comparable to that of *Sporosarcina pasteurii* (DSM 33). *Malays. J. Microbiol.* 463–470.
- Omeregje, A. I., Palombo, E. A., Ong, D. E., and Nissom, P. M. (2020). A feasible scale-up production of *sporosarcina pasteurii* using custom-built stirred tank reactor for *in-situ* soil biocementation. *Biocatal. Agric. Biotechnol.* 24, 101544. doi:10.1016/j.bcab.2020.101544
- Omeregje, A. I., Palombo, E. A., and Nissom, P. M. (2021). Bioprecipitation of calcium carbonate mediated by ureolysis: a review. *Environ. Eng. Res.* 26, 200379. doi:10.4491/eer.2020.379
- Omeregje, A. I., Muda, K., Bakri, M. K. B., Rahman, M. R., Yusof, F. A. M., and Ojuri, O. O. (2024). Calcium carbonate bioprecipitation mediated by ureolytic bacteria grown in pelletized organic manure medium. *Biomass Convers. Biorefinery* 14, 13005–13026. doi:10.1007/s13399-022-03239-w
- Osinubi, K., Eberemu, A., Gadzama, E., and Ijimdiya, T. (2019). Plasticity characteristics of lateritic soil treated with *Sporosarcina pasteurii* in microbial-induced calcite precipitation application. *SN Appl. Sci.* 1, 1–12. doi:10.1007/s42452-019-0868-7
- Özen, İ., and Şimşek, S. (2015). Vital importance of moisture level in all stages of processing from calcium carbonate coating through polyethylene/calcium carbonate compounding to film generation. *Powder Technol.* 270, 320–328. doi:10.1016/j.powtec.2014.10.038
- Park, S.-S., Le, T.-T., Nong, Z., Moon, H.-D., and Lee, D.-E. (2020). Chemically induced calcium carbonate precipitation for improving strength of sand. *J. Mater. Civ. Eng.* 32, 04020238. doi:10.1061/(asce)mt.1943-5533.0003318
- Payan, M., Sangdeh, M. K., Salimi, M., Ranjbar, P. Z., Arabani, M., and Hosseinpour, I. (2024). A comprehensive review on the application of microbially induced calcite precipitation (micp) technique in soil erosion mitigation as a sustainable and environmentally friendly approach. *Results Eng.* 24, 103235. doi:10.1016/j.rineng.2024.103235
- Pennock, D. (2019). *Soil erosion: the greatest challenge for sustainable soil management*. Rome, Italy: Food and Agriculture Organization.
- Ranjbar, F., and Jalali, M. (2015). The effect of chemical and organic amendments on sodium exchange equilibria in a calcareous sodic soil. *Environ. Monitoring Assessment* 187, 1–21. doi:10.1007/s10661-015-4894-7
- Safdar, M., Mavroulidou, M., Gunn, M., Purchase, D., Payne, I., and Garelick, J. (2021). Electrokinetic biocementation of an organic soil. *Sustain. Chem. Pharm.* 21, 100405. doi:10.1016/j.scp.2021.100405
- Shimobe, S., and Spagnoli, G. (2022). Relationships between strength properties and atterberg limits of fine-grained soils. *Geomechanics Geoenviron.* 17, 1443–1457. doi:10.1080/17486025.2021.1940317
- Stocks-Fischer, S., Galinat, J. K., and Bang, S. S. (1999). Microbiological precipitation of CaCO₃. *Soil Biol. Biochem.* 31, 1563–1571. doi:10.1016/s0038-0717(99)00082-6
- Sun, Y., Zhao, Q., Zhi, D., Wang, Z., Wang, Y., Xie, Q., et al. (2017). *Sporosarcina terrae* sp. Nov., isolated from orchard soil. *Int. J. Syst. Evol. Microbiol.* 67, 2104–2108. doi:10.1099/ijsem.0.001835
- Tourney, J., and Ngwenya, B. T. (2009). Bacterial extracellular polymeric substances (EPS) mediate CaCO₃ morphology and polymorphism. *Chem. Geol.* 262, 138–146. doi:10.1016/j.chemgeo.2009.01.006
- Umar, M., Kassim, K. A., and Chiet, K. T. P. (2016). Biological process of soil improvement in civil engineering: a review. *J. Rock Mech. Geotechnical Eng.* 8, 767–774. doi:10.1016/j.jrmge.2016.02.004
- Virto, I., Antón, R., Apesteguía, M., and Plante, A. (2018). “Role of carbonates in the physical stabilization of soil organic matter in agricultural mediterranean soils,” in *Soil management and climate change* (Elsevier), 121–136.
- Wu, S., Li, B., and Chu, J. (2021). Stress-dilatancy behavior of MICP-treated sand. *Int. J. Geomechanics* 21, 04020264. doi:10.1061/(asce)gm.1943-5622.0001923
- Wu, H., Xie, X., Xu, C., Liu, J., Zheng, X., and Zheng, L. (2024). Study on the effects and mechanism of the reinforcement of soft clay via microbially induced carbonate precipitation. *Appl. Sci.* 14, 7021. doi:10.3390/app14167021
- Xie, J., Gao, J., Cao, H., Li, J., Wang, X., Zhang, J., et al. (2024). Calcium carbonate promotes the formation and stability of soil macroaggregates in mining areas of China. *J. Integr. Agric.* 23, 1034–1047. doi:10.1016/j.jia.2023.09.015
- Zhang, Q., Ren, L., Sheng, Y., Ji, Y., and Fu, J. (2010). Control of morphologies and polymorphs of CaCO₃ via multi-additives system. *Mater. Chem. Phys.* 122, 156–163. doi:10.1016/j.matchemphys.2010.02.053